
Monitorization of Cleaning Processes from Digital Video Spatiotemporal Analysis. Cleaning Kinetics from Characteristic Times

[José Juan García-Jareño](#)^{*}, [Jerónimo Agrisuelas](#), Celia López, Fernando Lorenzo, [Francisco Vicente](#)^{*}

Posted Date: 13 January 2025

doi: 10.20944/preprints202501.0860.v1

Keywords: Surface cleaning characterization; Image analysis; Kinetics; Mean color intensity; Color variance



Preprints.org is a free multidisciplinary platform providing preprint service that is dedicated to making early versions of research outputs permanently available and citable. Preprints posted at Preprints.org appear in Web of Science, Crossref, Google Scholar, Scilit, Europe PMC.

Copyright: This open access article is published under a Creative Commons CC BY 4.0 license, which permit the free download, distribution, and reuse, provided that the author and preprint are cited in any reuse.

Article

Monitorization of Cleaning Processes from Digital Video Spatiotemporal Analysis. Cleaning Kinetics from Characteristic Times

José J. García-Jareño ^{1,*}, Jerónimo Agrisuelas ¹, Celia López ², Fernando Lorenzo ²
and Francisco Vicente ^{1,*}

¹ Physical Chemistry Department, Facultat de Química Universitat de Valencia, Dr. Moliner 50, 46100 Burjassot

² Christeyns España, C. Científica Margarita Salas Falgueras, 2, 46729 Ador, Valencia

* Correspondence: Jose.J.Garcia@uv.es (J.J.G.-J.); Francisco.Vicente@uv.es (F.V.)

Abstract: The cleaning process of metallic surfaces has been studied by means of digital video monitoring. Two theoretical models based on experimental observations are proposed for two possible cleaning mechanisms and two practical cases that can be adapted to these models are analyzed. As a kinetic parameter, the duration of the cleaning of a metallic surface is defined from the time evolution of the color intensities and their variance. These times allow us to characterize and to optimize the cleaning process procedure. Apparent activation energies are estimated from the characteristic times at different temperatures

Keywords: surface cleaning characterization; image analysis; kinetics; mean color intensity; color variance

1. Introduction

Generally, in chemical or food industry, metallic materials are commonly used to build tanks, reservoirs and pipes that connect them due to their high mechanical strength, good sealing and high durability. One of the advantages of this type of materials is that they can tolerate high temperatures or pressures and working conditions that are not possible with other, cheaper materials. Despite this important advantage, metallic materials also degrade and lose or change their properties over time since the metallic surfaces are continuously into direct contact with chemicals or foodstuffs[1–11]

Among many potential metallic alterations, corrosion must be controlled since it generates important losses. Degradation of the material and formation of oxides or hydroxides layers results in a loss of thermal conductivity (of special relevance in boilers and heat exchangers) or in the contamination of final products involving loss of quality in the case of chemical industry or food safety problems in the case of the food industry. For example, calcareous (calcium carbonate) deposits appear on the metal walls of systems when hard water is used, a process that is favored at high temperatures (over 45°C). To solve these problems, it is common to pre-treat the circulating water, using additives that prevent the precipitation of salts or cleaning with acidic products when the scale layer has already formed. In the food industry, the circulation and storage of organic matter facilitates the formation and growth of microorganisms that can form biological colonies, the so-called biofilms[12–21]. These biofilms act a reservoir of potentially damaging microorganisms that can contaminate the food product, but also affect the flow rates of circulating matter and the heat and electrical conductive properties of the metals in contact. The growth of biofilms requires scheduled shutdowns for periodic cleaning with the consequent economic cost that this demands for the company.

The cleaning process consists of a combination of chemical energy from cleaning products, temperature and mechanical action that allows to remove the remains from the metallic surface[22–

27]. Depending on the metallic materials, the chemical products must comply with a series of specifications, such as being non-corrosive, easy to dispose of, non-polluting and accelerating the cleaning process[26,28,29]. The potential environmental impact of the use of these products usually means that the minimum amount possible should be used under optimal temperature conditions. Therefore, the design of these cleaning products requires prior research work and laboratory experimentation to optimize the working conditions before applying them to any industrial installation[5,22,29–32].

Nowadays, evaluating and monitoring the cleaning process of a surface is not a standardized process due to the large number of applicable cases. It is important to consider that the cleaning process depends on many factors such as the type of residue or dirt to be removed, the environment in which it is found, the surface where it has adhered, etc.[2,29,33]. As a result, monitoring of the cleaning process may sometimes require the use of spectroscopic or electrochemical sensor based techniques [17,19,32,34–37].

At this point, we should consider the use of optical techniques as a first approach for the evaluation of the cleaning process of dirty surfaces. In recent years, the miniaturization of cameras (with or without smartphones) has been a revolution in the digital image acquisition systems since they can be coupled to tracking systems and they allow in situ monitoring for process control and decision making with a minimum margin of error[38–47]. Some advantages over other types of spectroscopic techniques are that it allows the simultaneous evaluation of the entire surface and not just a part of it, it requires a minimum investment, and the quality and speed of the cleaning process can be evaluated in situ and in the same facilities[48]. This simplifies the determination of the end point of the cleaning process and makes it considerably more straightforward to track the progress of the cleaning process at any given instant, as long as the illumination conditions are constant throughout the entire process.

For that purpose, it proves interesting the use of methodologies developed for the surface analysis during chemical changes involving color or homogeneity changes [39,44,49,50]. In each digital image, the color of any pixel corresponding to any part of the probe surface is a combination of 3 chromatic coordinates (Red, Green and Blue or RGB space) quantified by 256 intensity levels: I_R , I_G , and I_B . After separating the acquired video into individual frames, each pixel window of the studied surface area is converted in three data arrays, one per each color coordinate. For example, for an image of 100x100 pixels there will be a matrix of 10000 color intensity values for each coordinate at each instant. This means a large amount of information to be processed which can be summarized with two statistical parameters. For this purpose, from each array, the mean color intensity (\bar{I}_i) and variance of color intensity (sd_i^2) are calculated, one for each chromatic coordinate, where i represents the R, G or B color array.

$$\bar{I}_i = \sum_{j=1}^{n_p} \frac{I_i(j)}{n_p} \quad (1)$$

$$sd_i^2 = \frac{\sum_{j=1}^{n_p} (I_i(j) - \bar{I}_i)^2}{n_p} \quad (2)$$

where $n_p = n_v \times n_h$ is the total number of pixels of the analyzed area and depends on the number of vertical pixels (n_v) and the number of horizontal pixels (n_h).

Finally, three mean color intensities (eq. (1)) and three values for variance of color intensity (eq.(2)) are obtained per each digital image analyzed of all experimental course. On the one hand, the mean color intensity allows us to quantify the amount of surface that remains covered by a different color layer with a fine precision since an 8-bits camera discerns 256x256x256 possible colors (256 color levels per coordinate). On the other hand, the variance of the color intensity is a measure of the color dispersion and can also be interpreted as a measure of the quality and homogeneity of the surface. Besides, recent studies have revealed that the shape of the time evolution of variance curves during a surface color change process is directly related with the kinetic orders of the chemical process[44,49]. Therefore, we can consider these two parameters as excellent indicators to evaluate

and to quantify the time needed and the effectiveness of the cleaning process of a metallic surface under different experimental conditions.

In this work, we analyze two real case studies of cleaning processes by digital video through the time evolution of mean color intensity and color intensity variance. The aim is to characterize and quantify the cleaning process by digital video analysis which can be carried out to routine laboratory works with the intention to optimize the cleaning processes. The first one is the cleaning of a part of a stainless-steel pipe which presents an unknown black residue that seems to take place by a process of dissolution of the dirt layer without mechanical stirring. The second one corresponds to the cleaning of S316 stainless steel test probes with peanut butter studied in two concentrations of cleaning product, at two temperatures. To complete the peanut butter cleaning study, a flat vibrator fed continuously at 3 V and vibrating at 11000 rpm was applied to the steel plate as a mechanical action. In this research, we design a procedure able to monitor in a quantitative and qualitative way the cleaning process together with the development of precise theoretical models which allows us to understand and characterize the cleaning processes.

2. Materials and Methods

Metal samples consisted of a commercial stainless steel 316 pipeline and stainless steel 316 coupons of 6×1 cm, where an area of 2×1 cm was covered with peanut butter and the rest of the probe was covered with isolating Teflon tape.

The peanut butter was a commercial mark (Lucky Joe) and its composition, based on nutritional information provided in the label, is shown in **Table 1**.

Table 1. Peanut butter: summary nutritional information.

Nutritional information	Per 100g
Fats	51 g
Saturated fats	11 g
Carbohydrates	15 g
Sugars	8 g
Proteins	25 g
Salt (NaCl)	1.1 g

The cleaning products were provided by Christeyns. Two commercial detergents were used for this study. For the dissolution test of fatty residues such as peanut butter, MIDA FOAM 174 UW (MF174UW) was used. This product is a liquid foaming detergent with low alkalinity and great degreasing power. Its composition, based on non-ionic surfactants, organic solvents and sequestrants allows great cleaning power against organic residues and grease and mineral oils in food and beverage production environments. On the other hand, for the removal of the black residue BETELENE MS-NP (BMSNP) was used. It is an acid descaling detergent based on methanesulphonic acid as active ingredient. Methanesulphonic acid is a sustainable alternative to conventional acids used in detergency. These detergents contain a mixture of surfactants, sequestering agents, solvents and specific acidic or alkaline raw materials for the complete removal of the protein, fat and carbohydrate content of the chosen residue. The safety data sheet and technical information for each tested product describes its main properties and characteristics[51]. These products were used in dilutions of 5% BMSNP and 1% or 3% for MF174UW. The water for these dilutions was ultrapure water (18 MOhms cm). The mechanical action was simulated by applying a flat vibrator (DC3V 80 mA 11000 rpm, 0.8 cm² surface area) to the steel sample immersed in a detergent solution. The temperature at which the prepared dilutions were applied was 20 °C and 40 °C. It was measured with a sensitivity of 0.1 °C and was controlled by means of a heating plate, obtaining a stable temperature with variations during the experiment of less than 0.5 °C.

The acquisition of digital images was carried out with the help of a digital camera (EPA-503278) with a resolution of 640×480 pixels and 24 bits of color deep in RGB space. Images were sequentially

recorded at each time interval, adapting to the expected speed of the cleaning process (**Figure 1**). After the acquisition of the images and with the help of proprietary software, the mean color intensity for the RGB coordinates and their variance in the studied region of the surface was obtained for each one of the images (**Figure 2**).

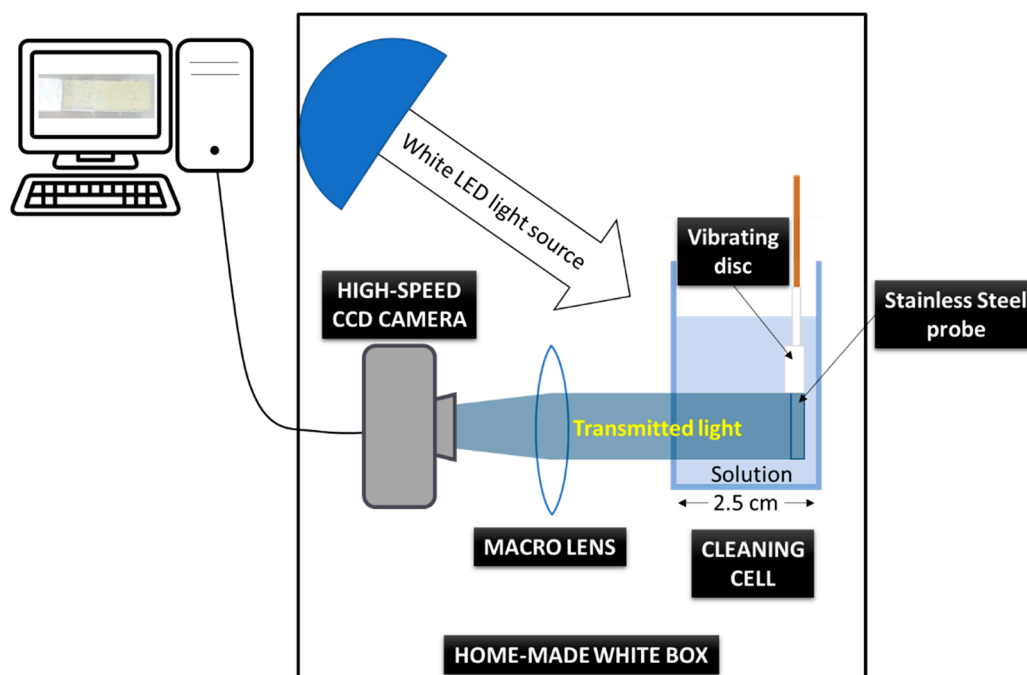


Figure 1. Schema of the digital video acquisition during the cleaning process.

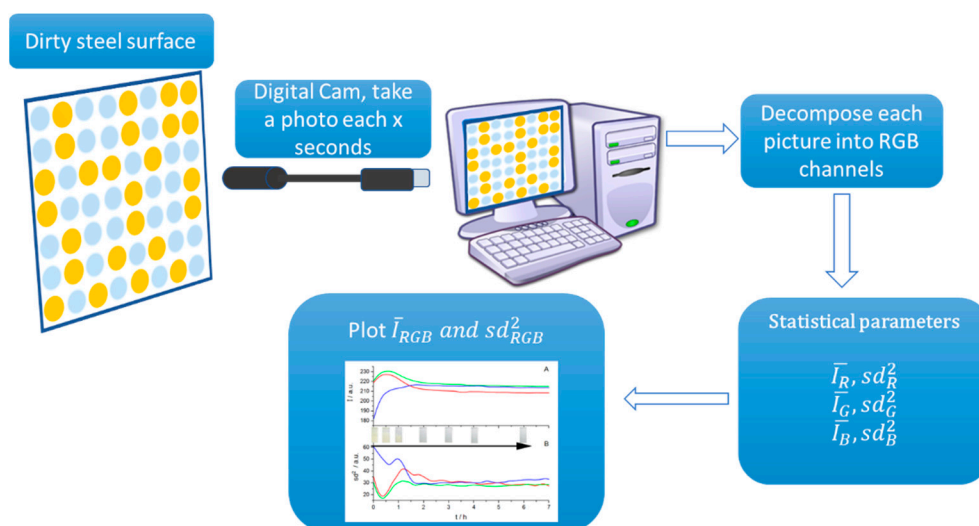


Figure 2. Workflow to obtain mean color intensities and variance from the color image acquired.

Modelization

First, let us consider two simplified and ideal models by which the cleaning process can take place and the expected digital image results for each process. This section will allow us to better understand the experimental results obtained in real samples.

In the first model, the cleaning takes place by the chemical attack of the detergent product with the consequent complete dissolution of the deposited soiling, layer by layer. From the point of view of surface color change, the cleaning process will show an apparent latency period without any color change despite of the dissolution process taking place, since the dissolution of the outermost layers of dirt exposes a new layer of dirt with the same surface color and homogeneity, but with a decreasing

thickness. At certain moment, the last layer of dirt begins to disappear, exposing the bare metal surface. We can define this time as $(t_{0,s})$, the first time at which the metal surface appears.

This process results in changes of color homogeneity and intensity of the image due to the emergence of new colored pixels. The change in the mean color intensity can be both positive or negative depending on the color of the dirt layer and the bare metal surface. The variance always increases initially since the metal surface is more and more exposed and at least two different color surfaces appear simultaneously. Variance reaches a maximum value, which is interpreted as the point where the color dispersion is maximum. In other words, this is the time at which half of the metal surface is covered by the layer of dirt and the other half is clean. We call this time the half-life time of surface cleaning process $(t_{1/2})$. It is important to note that this time is not the half-life time of the complete cleaning process since it depends on the thickness of the dirt layer. From this point on, the dirt layer will continue to dissolve, and the color of the metal surface will increasingly prevail, making the surface more homogeneous and thus decreasing the variance. In an ideal situation, at the end the entire surface is clean and will be identified by the fact that the average color intensity no longer changes, and the variance has returned to a minimum value. This is the end time or final time of the cleaning process (t_f) .

Figure 3 shows two simulations of how these parameters (mean color intensity and color intensity variance) evolve over time for a cleaning process considering this dissolution mechanism and assuming that the analyzed region of the image of n_p pixels changes its color between a color intensity I_1 characteristic of the dirt layer to a final color intensity I_2 , characteristic of the clean metal surface. We also suppose an irreversible process governed by a kinetic constant k_1 . Mechanical action, such as stirring the dissolution, can accelerate the process by removing from the metal surface the solvent layers more concentrated in dirt. The shape of these curves is characterized by the equations collected in **Table 2**[44,46]. The mean color intensity (\bar{I}) , the variance sd^2 , the peak widths $(\omega_{1/2})$, the peak half-widths $(\omega_{1/4}$ left and right side) and the ratio between the peak half widths of variance peaks depends on the kinetic orders (0,1,2) [41,44]. It should be noted that this last ratio can be interpreted as a measure of the symmetry of variance peaks. In accordance with **Table 2**, these peaks will show a symmetrical shape only for kinetics of order 0, while for kinetics of higher orders, the right side of the peak appears wider than the left side[41,44].

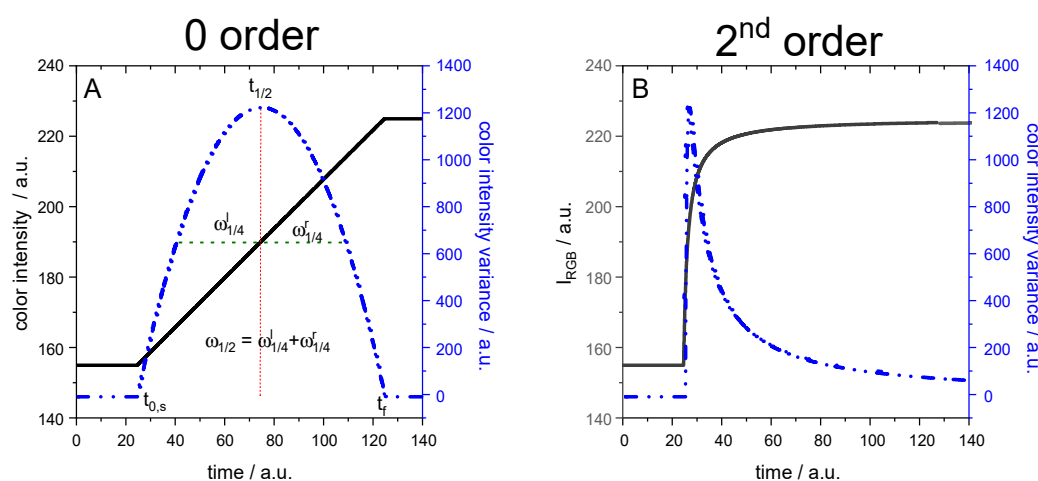


Figure 3. Simulation of the evolution of mean color intensity and variance against the elapsed time, in arbitrary measurement units, during a surface chemical reaction for a zero-order reaction (A) and second order reaction (B) [44].

Table 2. Peak widths ($\omega_{1/2}$) and half peak widths ($\omega_{1/4}$) of variance versus time for different kinetic orders. n_p is the number of pixels in the image, I_1 is the mean color intensity characteristic of the dirt layer, I_2 is characteristic of the clean metal surface and k is the kinetic constant of the irreversible process of cleaning[44].

Order	\bar{I}	sd^2	$\omega_{1/2}$	$\omega_{1/4}^r$	$\omega_{1/4}^l$	$\frac{\omega_{1/4}^r}{\omega_{1/4}^l}$
0	$I_1 + \frac{I_2 - I_1}{n_p} k_1 t$	$\frac{k_1(I_2 - I_1)^2(n_p - k_1 t)t}{n_p^2}$	$\frac{n_p}{k_1 \sqrt{2}}$	$\frac{n_p}{k_1 \sqrt{8}}$	$\frac{n_p}{k_1 \sqrt{8}}$	1
1	$I_2 + \frac{(I_1 - I_2)}{e^{k_1 t}}$	$\frac{(e^{k_1 t} - 1)(I_2 - I_1)^2}{e^{2k_1 t}}$	$\frac{1.76}{k_1}$	$\frac{1.23}{k_1}$	$\frac{0.53}{k_1}$	2.3
2	$\frac{k_1 t(I_2 - I_1)^2 n_p}{(k_1 t n_p + 1)^2}$	$\frac{k_1 t(I_2 - I_1)^2 n_p}{(k_1 t n_p + 1)^2}$	$\frac{5.66}{k_1 n_p}$	$\frac{4.83}{k_1 n_p}$	$\frac{0.83}{k_1 n_p}$	5.8

(r) and (l) refers to the right part and the left part of the variance peak, respectively.

In the second proposed mechanism, the cleaning product chemically attacks the layer of dirt changing both the mechanical properties and the adhesion to the metal surface. The layer of dirt will eventually become easier to peel off from the metal surface and easier to break off. Therefore, this proposed mechanism necessarily adds to the chemical cleaning some mechanical actions when dirt is removed in portions.

This second proposed mechanism also starts with a chemical attack on the surface of the deposited dirt layer that does not necessarily involve the dissolution of the dirt layer. In some cases, the chemical attack will involve a change in the physical-chemical properties of the layer of dirt which can be observed as a color change of the layer of dirt. Therefore, we would observe changes in color intensity from the original color to the color of the coating after the chemical attack and a peak in the evolution over time of the variance[44] similar to that simulated in **Figure 3**.

Once the chemical attack has occurred, the mechanical action removes this layer of dirt from the surface of the metal and both the mean color intensity, and the variance will show irregular evolutions until the clean metal surface appears. These irregularities can be masked if the surface area studied is large enough and the pieces of dirt leaving the surface are not very large size. Note that this process and its speed will be totally dependent on the type of mechanical action and its extent. As the layer of dirt is not dissolved, portions of dirt pass to the solution as a suspension or precipitate, depending on the relative density of the dirt. In the case of no mechanical action applied, in this type of cleaning mechanism, the removal of the layer of dirt from the metal surface may not occur and it may remain weakly adhered to the metal probe. Finally, it would be possible to partially recover the cleaning solutions by a filtering process which will eliminate the solid fragments of dirt, allowing them to be reused in subsequent cleaning.

3. Results and Discussion

3.1. Cleaning by Dissolution

In the first case, a piece of an industrial pipe showing with a blackish layer of dirt caused by their normal use and of unknown composition was cleaned by immersion in an aqueous solution of BMSNP (5%) whose active ingredient was a methanesulphonic acid solution, without mechanical stirring during 24 h. An accelerated video of this cleaning process can be seen in Video S1 (supplemental material).

The time evolution of mean color intensity for the three colors and the corresponding color intensity variance of the whole pipe surface is depicted in **Figure 4**. During the first two hours, a small increase in the color intensities was observed (**Figure 4A**). This may be due to the beginning of the chemical attack of the cleaning product on the stain, or to a simple hydration of the outermost layer. The first significant color changes on the surface are observed at times between 8 and 12 hours,

when the surface of the uncoated metal begins to appear ($t_{0,s}$). These color changes continue until 18 hours (t_f), when it is observed that the color intensities hardly change with time, which corresponds to the surface of the metal being now clean. Regarding the time evolution of variance, a peak appears at about 15.5 hours which corresponds to the time where one half of the analyzed pipe surface keeps black, and the other half shows the final white-grey color ($t_{1/2}$, **Figure 4B**). Previously to this peak, a shoulder at about 9 hours was observed. This behavior can be explained by the fact that the analyzed surface is large enough and the dirt layer proves not homogeneous in thickness or chemical composition (See EDX microanalysis data in Figure S1, supplemental material).

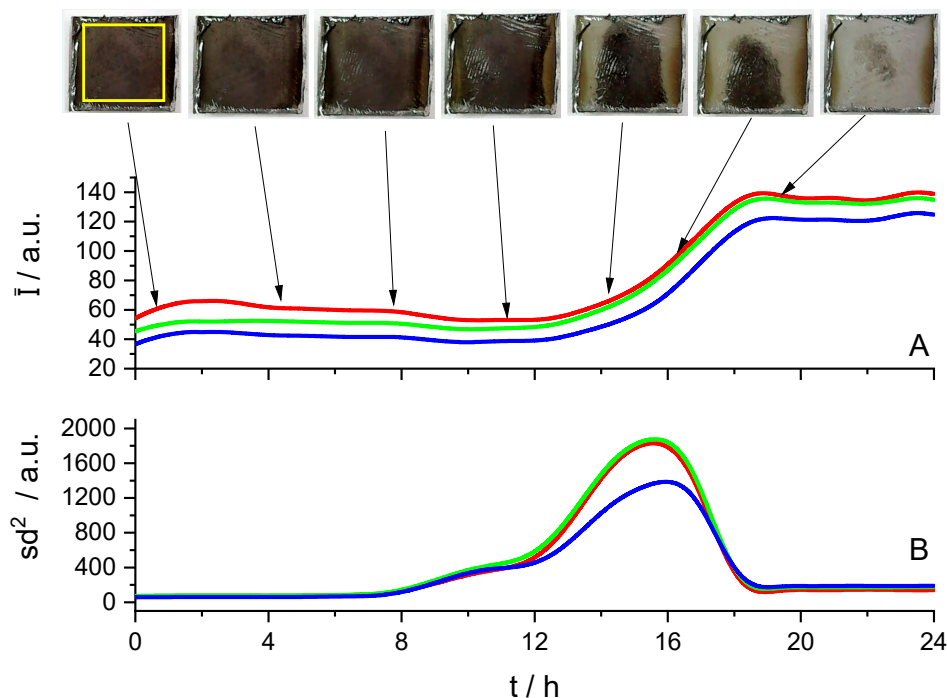


Figure 4. Evolution with time of mean color intensity and variance during the cleaning of a piece of pipe with a methanesulphonic acid-based product BMSNP (5%). The yellow rectangle in the leftmost image indicates the analyzed area.

One of the advantages of digital video analysis is the simultaneous spatiotemporal study of different areas of the test probe. Due to the non-homogeneity of the dirt on the pipe surface, we proceed to study the evolution of these kinetic parameters in two regions of the sample marked as 'upper left' and 'lower right' in **Figure 5**. Compared with data in **Figure 4**, we observe that the cleaning of the last layer of dirt starts around 12 hours ($t_{0,s}$) on the left side of the sample. After that, we observe that the maximum and constant color intensity of the left side is reached at about 16 hours, at relatively shorter times than for the case of the entire surface. Something similar is observed for the evolution of the variance with time. In this last case, the shape of the variance peak looks more symmetrical than the peaks obtained from the right side or for the whole metal surface analyzed. This result can be explained by a more homogeneous region analyzed on the left side of the sample. Also, the peak for the maximum occurs at 14.5 hours, 1 hour before the maximum for the whole surface analysis. Looking now at the right side of the sample, a steeped decrease of color intensities is observed between 7h and 12 h. This means that the surface is becoming darker. A possible explanation is that the first hydrated layer has been removed and the innermost layer of dirt is visible. After 12 hours the color intensity increases for the three coordinates until it reaches a maximum and constant value at about 18 hours. Once the surface is clean, changes are not very significant. For the

evolution of the variance over time, minimal changes occur before 12 hours, then an increase to define a peak with a maximum value just before 16 hours, a sharp decrease and from 18 hours onwards there is hardly any change.

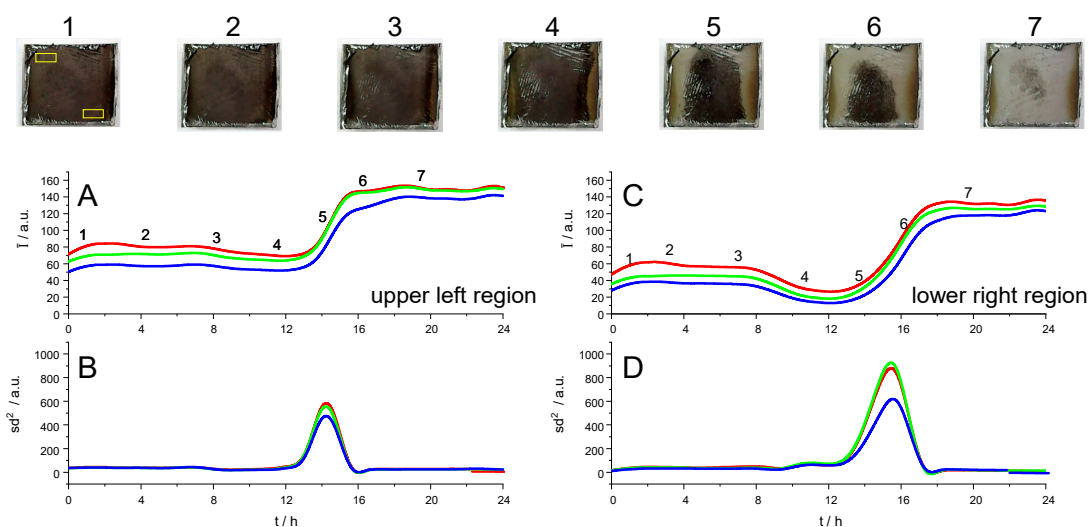


Figure 5. Evolution with time of mean color intensity and variance during the cleaning of a piece of pipe with a methanesulphonic acid-based product BMSNP (5%). Graphs A) and B) correspond to the upper left region and graphs C) and D) correspond to the lower right region marked in yellow of the leftmost image.

Table 3 shows the values obtained for the characteristic times and peak half-widths of variance for the three regions analyzed. First, if we analyze the values of the characteristic times, we can note that they are lower in the left region than in the right region or the global measurement. In particular, the half-life time appears 1.2 hours earlier in the left region. A second observation involves the peak width and half-widths. For the left region, significantly lower values are observed confirming that the analyzed region was more homogeneous than in the other two cases. Finally, the ratio of the peak half-widths is close to unity in all three cases, somewhat smaller for the study of the entire surface. According to previously published models these values near the unity can be interpreted as an order 0 kinetics for this cleaning process.

Table 3. Characteristic times for the cleaning of a piece of pipe with a methanesulphonic acid-based product BMSNP (5%) on different parts on the sample extracted from **Figure 4** and **Figure 5**.

Region	t_0 / h	$t_{1/2}$ / h	t_f / h	$\omega_{1/4}^l$ / h	$\omega_{1/4}^r$ / h	$\omega_{1/4}^r/\omega_{1/4}^l$
Upper left	12.4	14.2	16	0.9	0.8	0.95
Lower right	12.5	15.4	16.5	1.3	1.2	0.92
Global	11.5	15.6	18.7	2.5	1.7	0.70

To observe these differences in better detail, a 3D map of color variation versus time and distance from the left end of the sample is presented [43]. As a representative result, **Figure 6** shows the 3D map of mean color intensity and variance of red color. Several observations can be drawn from **Figure 6**. On the one hand, for longer times the color of the surface is not homogeneous, a lower color intensity being observed in the central part, which means that it is somewhat more blackened than the ends. On the other hand, the isochromatic lines are not horizontal, but follow an inverted U-shape, indicating that the central part changes its color later than the periphery. Another interesting observation is that the isochromatic lines are closer together in the central region of the metal than in the outer regions. This distance between isochromatic lines is directly related to the rate of color

change. Therefore, once the last layer has begun to disappear in the central region, the dissolution rate appears to be somewhat higher than the dissolution rate in the outer zones. If we analyze the 3D plot of the evolution of the color variance against the elapsed time and the distance to the left boundary of the sample, we can remark some points. First, changes in variance do not take place gradually but occur when the dissolution of the last layer of dirt occurs and the color of the metal is observed. As predicted by the theoretical models for the evolution of the variance over time, it is observed that the variance initially increases when the dissolution of the last layer begins, reaches the maximum value, and finally decreases as the observed surface becomes more homogeneous again. This maximum corresponds to the characteristic half-life time $t_{1/2}$ previously defined. Note that this time is not the same for any position on the sample under study but shows higher values in the central region and lower values at the outer sides. Note also how at this point, the central region shows higher variance values for times greater than 18 hours than the variance at the outer sides. This is because there are remains of the dirt layer after 24 hours in the central region, while the outer sides appear cleaner. Other interesting observations are that variance changes begin at shorter times at the outer sides, and the homogeneous color is also reached earlier in these regions.

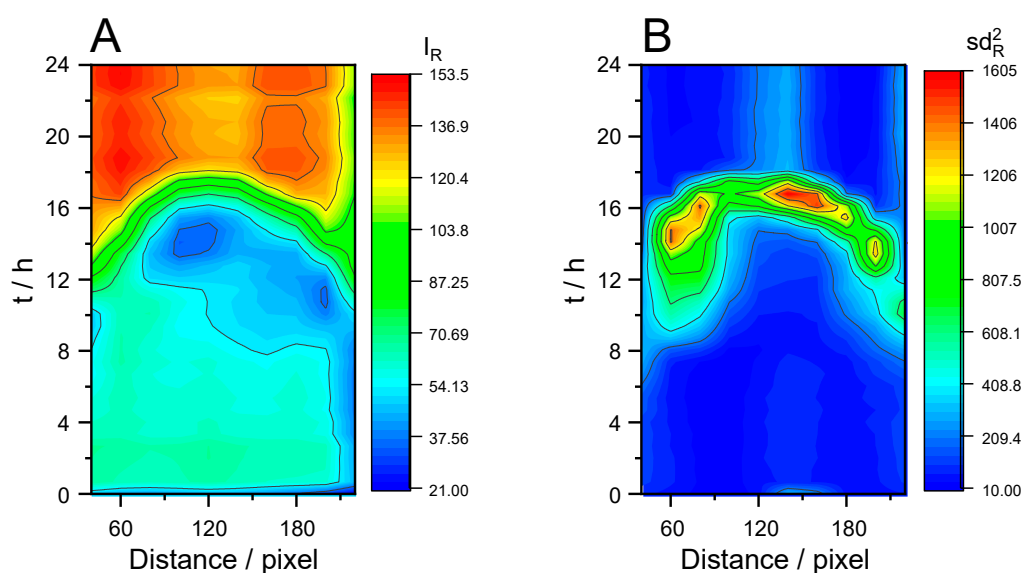


Figure 6. 3D plots of mean color intensity (A) and variance of color intensity of red color (B) against the elapsed time and the distance in pixels from the left side of the analyzed sample in a methanesulphonic acid-based product BMSNP (5%).

3.2. Peeling Off Cleaning

In the second case, chemical attack on the layer of dirt was combined with mechanical action. For this purpose, we studied the cleaning of steel plates on which 0.28 g of peanut butter has been previously spread. The steel plate was submitted to the action of a flat vibrator at 11000 rpm during the cleaning process.

To study the effect of the cleaning product on the peanut butter residue, this cleaning process was followed by the acquisition of sequential images during the necessary time until the entire surface was cleaned. The original mean color of the peanut butter in our lighting conditions is ocher (230,222,193) (image 1 in **Figure 7**), changing after a short time and after the chemical attack to a quite intense white color (250,250,240) (image 2 in **Figure 7**). Therefore, color increments of (20,28,47) units for each color coordinate were observed. This makes the changes more evident in the blue coordinate than in red or green, although they are also noteworthy for these coordinates. After the test was completed, when the steel plate was removed from the cleaning solution, it was observed that the peanut butter layer had a gelatinous appearance, its volume had increased considerably, the color

was much whiter and it easily peeled off the surface in the form of a film (image 3 in **Figure 7**). An accelerated video of this process can be seen in the supplementary material. (Video S2).

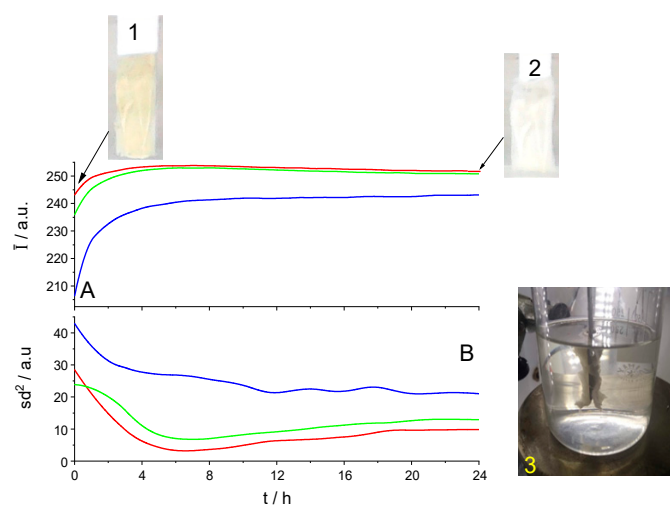


Figure 7. Color intensity and variance changes during the chemical attack process of MF174UW (1%) peanut butter product on S316 stainless steel. Peanut butter sample before (image 1) and after 24 hours (image 2 and 3).

Figure 7 shows how the chemical attack of the cleaning product MF174UW takes place during the first 4-6 hours until the mean color intensity (**Figure 7A**) and its variance (**Figure 7B**) reach almost constant values for the three colors. Unexpectedly, the variance does not show a peak as in theory (**Figure 3**) for the change from the ochre color (image 1 in **Figure 7A**) to white (image 2 in **Figure 7A**). We can explain this fact considering that the initial color dispersion for the steel surface coated with peanut butter is high enough due to spreading procedure of peanut butter which cause a non-homogeneous layer and some shadows are formed in our lighting conditions. Therefore, we observe only a decrease from the inhomogeneous color of the peanut butter to the more homogeneous color of the chemically attacked layer. On the other hand, the 3D plots of mean red color intensity and its variance against the elapsed time and the distance in pixels from the top of the metal sample (**Figure 8**) show that the color changes occur earlier and more extensively on the bottom of the metal plate. However, the swelling of the peanut butter can affect the quality and accuracy of these observations (image 3 in **Figure 7**).

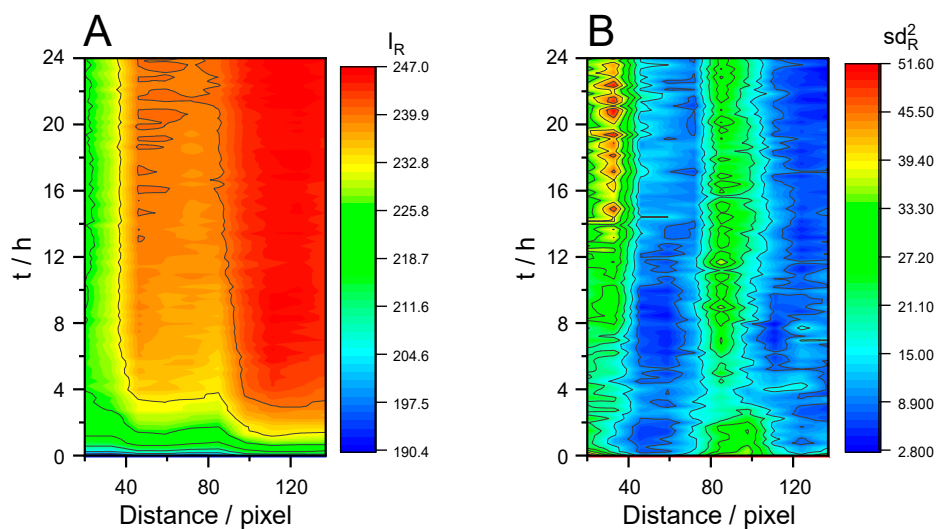


Figure 8. 3D plots of mean color intensity (A) and variance (B) of red color during chemical attack of MF174UW (1%) on peanut butter on S316 steel plate.

In the following experiment, we have added the effect of mechanical action generated by a flat vibrating motor at 11000 rpm during the chemical peanut butter cleaning. In supplemental material there is an accelerated video corresponding to this experiment. For the same composition (1% MF174UW), the chemical attack of the cleaning product is also observed since there is a color change from ocher to white (**Figure 9**). After the chemical attack, some fragments peel off from the peanut butter. In terms of color change, the blue color hardly changes in this last step, but the intensity of red and green decreases as the surface of the steel becomes darker (**Figure 9A**).

The variance evolution for the three colors over time (**Figure 9B**) shows the effect of chemical attack during the first 30 minutes as before due to the bleaching of peanut butter. Then, a peak appears in the three coordinates, but not synchronously. The maximum for blue appears earlier than for the other two colors caused by the change from ocher to white which involves the greatest increase in the blue coordinate (**Figure 9A**). Thus, red and green variance peaks proved more appropriated to study the cleaning process since in this case, changes of variance are mainly due to changes from the white chemically attacked peanut butter to the white-grey of the bared steel surface. The peak observed for green and red color around 75 minutes corresponds to the time when one half of the surface keeps covered by peanut butter and the other half uncovered. Careful observation of the shape of the red color variance shows that it is quite asymmetrical, as corresponds to first or second kinetic orders (see **Figure 3**). Due to overlapping of two processes (chemical attack and peeling off), the resulting shape of these curves does not allow an accurate estimation of the half width at half maximum to discern between first and second kinetic order (**Table 2**), but we can discard a zero-order kinetics reaction. An accelerated video of this process can be seen in the supplementary material (Video S3).

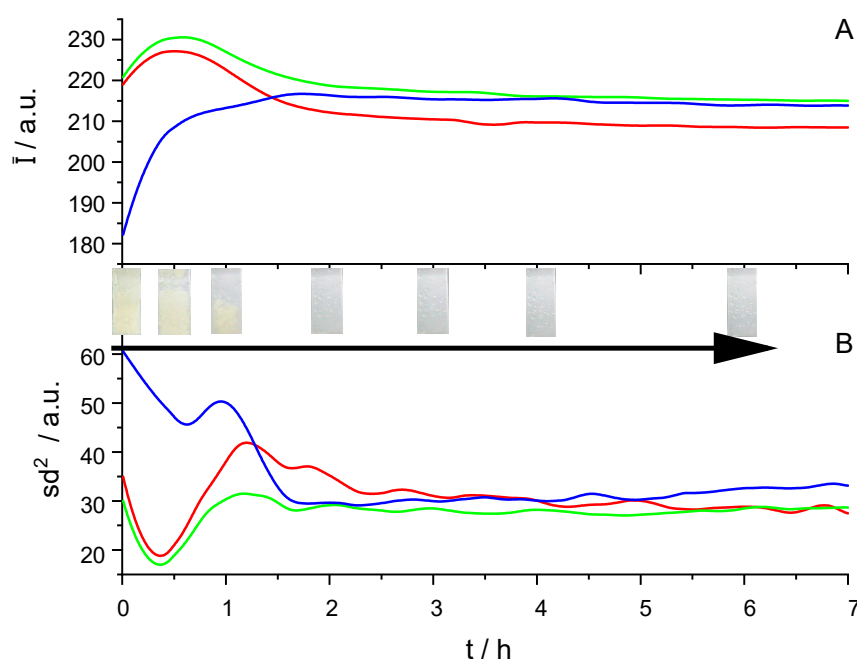


Figure 9. The time evolution of mean color intensity and variance of color intensity during the cleaning process of peanut butter on a steel plate with mechanical vibration. (1% MF174UW, 20 °C, vibration 11000 rpm).

At higher concentration of the cleaning agent (3% of MF174UW), we expect an acceleration of the cleaning process. Initially, the first color change to white is not observed. If we assume that the

chemical attack takes place faster, then it is possible that the breakage and loss of adhesion to the metal may take place before the color change of this surface. 3D plots of blue color intensity and their variance against the elapsed time and the distance from the top of the electrode are presented in **Figure 10**. For the blue color intensity, one can observe that before 30 min the final color was reached (**Figure 10A**). The maximum of variance is reached at different parts of the steel plate at about 15 minutes without many differences with the distance from the top of the electrode (**Figure 10B**). The mechanical action of the vibration, together with the higher concentration of the cleaning product smooth the changes of observed colors.

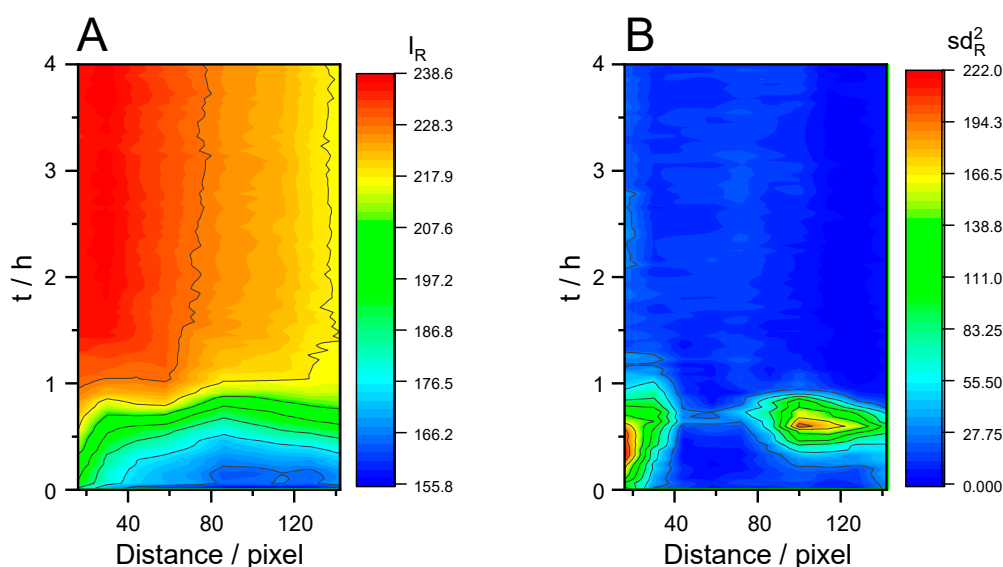


Figure 10. 3D plots of mean color intensity and variance against time and distance in pixels from the top of the steel plate with mechanical vibration (3% MF174UW , 20°C and vibration 11000 rpm).

Table 4 summarizes the results of the cleaning process at two temperatures, for two concentrations of the cleaning product and applying or not vibration as a mechanical action that helps the cleaning of the product. **Table 4** allows us to corroborate that increasing the concentration of the cleaning product from 1% to 3% multiplies the cleaning speed by approximately two. It can be assumed that under the experimental conditions of this work, with the use of the vibrating electrode, it is possible to renew the solution in the vicinity of the peanut butter layer continuously. Therefore, the MF174UW concentration will remain constant. If we consider a simplified model in which the cleaning rate depends on both, the surface concentration of dirt (Γ_d) and on the solution concentration of MF174UW ($[MF174UW]$), we can write a rate equation as:

$$rate = k_1 \Gamma_d^\alpha [MF174UW]^\beta = k_{ap} \Gamma_d^\alpha \quad (3)$$

$$k_{ap} = k_1 [MF174UW]^\beta \quad (4)$$

Therefore, if the concentration is multiplied by 3 and the speed (estimated from t_{end} in **Table 4**) by (1.6-2.5), this means an experimental apparent kinetic order β for MF174UW of 0.4-0.8.

We can also estimate the temperature effect on the cleaning rate, an increase from 20 °C to 40 °C reduces the cleaning times by approximately 2-3 times and this allows us to estimate the apparent activation energy of the cleaning process, assuming an Arrhenius dependence of kinetics constant on the temperature (about 25-40 kJ mol⁻¹).

Table 4. Characteristic times for the cleaning process of peanut butter on steel with the product MF174UW in concentrations of 1% and 3%, at a temperature of 20 °C and 40 °C and without mechanical action and with mechanical action (vibration).

Conditions for the cleaning process			1 st process (whitening)			2 nd process (peeling off)		
T / K	Vibration	Conc. (%)	t_0 / s	$t_{1/2}$ / s	t_{end} / s	t_0 / s	$t_{1/2}$ / s	t_{end} / s
293	NO	1%	160		2255			
293	NO	3%	20		1280			Not observed
293	YES	1%				810	1240	2030
293	YES	3%		Not observed		0	500	1270
313	NO	1%	0		4000			Not observed
313	NO	3%		Not observed		902	2058	2556
313	YES	1%				460	750	1040
313	YES	3%		Not observed		0	177	414

4. Conclusions

Monitoring of color changes during the cleaning process of a metal surface by digital images allows not only qualitative but also quantitative evaluation of the efficacy and kinetics of the cleaning process. The use of spatio-temporal data analysis for this purpose is a great advantage over other forms of online monitoring of the cleaning process as it allows the homogeneity of the entire surface and the final quality of the process to be evaluated.

The characteristic times defined from the curves of color intensities and variance evolution versus the time are excellent indicators not only of the rate of the process, but also of the final quality of the cleaning process. The analysis of these parameters shows how the cleaning process is quantitatively affected by the concentration of the cleaning product, the temperature and the mechanical action exerted, even estimating an activation energy for the cleaning process. Finally, this type of analysis allows us to obtain an initial estimation of the kinetics of the cleaning process, which can be used to estimate the time needed to finish the cleaning process and, based on this, to optimize the experimental conditions .

Supplementary Materials: The following supporting information can be downloaded at the website of this paper posted on Preprints.org, Figure S1: EDX Microanalysis at different points on the sample surface; Video S1: Accelerated video of the cleaning process by a dissolution mechanism. Video S2: Accelerated video of the cleaning process of a steel sample covered by peanut butter without mechanical vibration. Video S3: Accelerated video of the cleaning process of a steel sample covered by peanut butter with mechanical vibration.

Author Contributions: C.L.F.L., J.A., J.J.G.-J. and F.V.: Conceptualization, methodology, validation, formal analysis, resources, data curation, writing—original draft preparation, writing—review and editing, visualization, project administration, funding acquisition. All authors have read and agreed to the published version of the manuscript.

Funding: This research was funded by AVI, Agencia Valenciana de la Innovación (Valencian Innovation Agency) in the program for the promotion of talent in line 3 of action, for the support of research personnel in companies for the completion of doctoral theses with the European regional development fund in the INNTA3/2021/24 “Research into corrosive processes and the accumulation of residues on metal surfaces and the development of preventive hygienic designs for cleaning and disinfection operations” ; Spanish E3TECH-PLUS Research Network GRANT number RED2022-134552-T “Aplicaciones Medioambientales y Energeticas de la Tecnologia Electroquimica Frente a los Retos del Nexa Agua-Energia” and The APC was waived by invitation.

Data Availability Statement: The data presented in this study are available on request from the corresponding author due to future collaborative research projects.

Acknowledgments: SEM and EDX were carried out in the Microscopy Section of Central Service for Experimental Research (SCSIE) of the University of Valencia.

Conflicts of Interest: The authors declare no conflicts of interest.

References

1. Pontefract, R. Bacterial Adherence - Its Consequences in Food-Processing. *Canadian Institute of Food Science and Technology Journal-Journal De L Institut Canadien De Science Et Technologie Alimentaires* **1991**, *24*, 113–117, doi:10.1016/S0315-5463(91)70033-3.
2. Boulané-Petermann, L. Processes of Bioadhesion on Stainless Steel Surfaces and Cleanability: A Review with Special Reference to the Food Industry. *Biofouling* **1996**, *10*, 275–300, doi:10.1080/08927019609386287.
3. Jackson, L.S.; Al-Taher, F.M.; Moorman, M.; DeVries, J.W.; Tippett, R.; Swanson, K.M.J.; Fu, T.-J.; Salter, R.; Dunaif, G.; Estes, S.; et al. Cleaning and Other Control and Validation Strategies to Prevent Allergen Cross-Contact in Food-Processing Operations. *J Food Prot* **2008**, *71*, 445–458, doi:10.4315/0362-028x-71.2.445.
4. Rossi, S.; Leso, S.M.; Calovi, M. Study of the Corrosion Behavior of Stainless Steel in Food Industry. *Materials* **2024**, *17*, 1617, doi:10.3390/ma17071617.
5. Chung, M.M.S.; Tsai, J.-H.; Lu, J.; Padilla Chevez, M.; Huang, J.-Y. Microbubble-Assisted Cleaning To Enhance the Removal of Milk Deposits from the Heat Transfer Surface. *ACS Sustainable Chem. Eng.* **2022**, *10*, 8380–8387, doi:10.1021/acssuschemeng.2c01194.
6. Dallagi, H.; Jha, P.K.; Faille, C.; Le-Bail, A.; Rawson, A.; Benezech, T. Removal of Biocontamination in the Food Industry Using Physical Methods; an Overview. *Food Control* **2023**, *148*, 109645, doi:10.1016/j.foodcont.2023.109645.
7. Passive Reflectance Sensing and Digital Image Analysis for Assessing Quality Parameters of Mango Fruits | Elsevier Enhanced Reader Available online: <https://reader.elsevier.com/reader/sd/pii/S0304423816304976?token=6A7270E7996BFE73CC6C0A21819BD3FC5AC30753A16BFE0F65A1414EC545A00E2FE7BDA4E662A45877A18FD001382575> (accessed on 19 April 2019).
8. Alonso, V.P.P.; Lemos, J.G.; Nascimento, M. da S. do Yeast Biofilms on Abiotic Surfaces: Adhesion Factors and Control Methods. *International Journal of Food Microbiology* **2023**, *400*, 110265, doi:10.1016/j.ijfoodmicro.2023.110265.
9. Crandall, P.G.; O'Bryan, C.A.; Wang, D.; Gibson, K.E.; Obe, T. Environmental Monitoring in Food Manufacturing: Current Perspectives and Emerging Frontiers. *Food Control* **2024**, *159*, 110269, doi:10.1016/j.foodcont.2023.110269.
10. Gomes, L.C.; Saubade, F.; Amin, M.; Spall, J.; Liauw, C.M.; Mergulhão, F.; Whitehead, K.A. A Comparison of Vegetable Leaves and Replicated Biomimetic Surfaces on the Binding of *Escherichia Coli* and *Listeria Monocytogenes*. *Food and Bioprocess Processing* **2023**, *137*, 99–112, doi:10.1016/j.fbp.2022.11.003.
11. Wan Omar, W.H.; Mahyudin, N.A.; Azmi, N.N.; Mahmud Ab Rashid, N.-K.; Ismail, R.; Mohd Yusoff, M.H.Y.; Khairil Mokhtar, N.F.; Sharples, G.J. Effect of Natural Antibacterial Clays against Single Biofilm Formation by *Staphylococcus Aureus* and *Salmonella Typhimurium* Bacteria on a Stainless-Steel Surface. *International Journal of Food Microbiology* **2023**, *394*, 110184, doi:10.1016/j.ijfoodmicro.2023.110184.
12. Chmielewski, R. a. n.; Frank, J. f. Biofilm Formation and Control in Food Processing Facilities. *Comprehensive Reviews in Food Science and Food Safety* **2003**, *2*, 22–32, doi:10.1111/j.1541-4337.2003.tb00012.x.
13. Orihuel Iranzo, E.; Bertó Navarro, R.; Lorenzo Cartón, F.; López Tormo, C.; San José Serran, C.; Orgaz Martín, B. Biofilm-Marking Composition and Method for Detection of Same on Surfaces 2013.
14. Cappitelli, F.; Polo, A.; Villa, F. Biofilm Formation in Food Processing Environments Is Still Poorly Understood and Controlled. *Food Eng. Rev.* **2014**, *6*, 29–42, doi:10.1007/s12393-014-9077-8.
15. Galié, S.; García-Gutiérrez, C.; Miguélez, E.M.; Villar, C.J.; Lombó, F. Biofilms in the Food Industry: Health Aspects and Control Methods. *Frontiers in Microbiology* **2018**, *9*.
16. Kabwanga, I.T.; Yetişemiyen, A.; Nankya, S. Dairy Industrial Hygiene: A Review on Biofilms Challenges and Control. *International Journal of Research -GRANTHAALAYAH* **2018**, *6*, 268–273, doi:10.29121/granthaalayah.v6.i2.2018.1570.

17. Puga, C.H.; Dahdouh, E.; SanJose, C.; Orgaz, B. *Listeria Monocytogenes* Colonizes *Pseudomonas Fluorescens* Biofilms and Induces Matrix Over-Production. *Front. Microbiol.* **2018**, *9*, doi:10.3389/fmicb.2018.01706.
18. Lorenzo, F.; Sanz-Puig, M.; Bertó, R.; Orihuel, E. Assessment of Performance of Two Rapid Methods for On-Site Control of Microbial and Biofilm Contamination. *Applied Sciences* **2020**, *10*, 744, doi:10.3390/app10030744.
19. Brozkova, I.; Cervenka, L.; Motkova, P.; Fruhbauerova, M.; Metelka, R.; Svancara, I.; Sys, M. Electrochemical Control of Biofilm Formation and Approaches to Biofilm Removal. *Appl. Sci.-Basel* **2022**, *12*, 6320, doi:10.3390/app12136320.
20. Sha, J.; Xu, C.; Xu, K. Progress of Research on the Application of Nanoelectronic Smelling in the Field of Food. *Micromachines* **2022**, *13*, 789, doi:10.3390/mi13050789.
21. Zhang, X.; Yang, C.; Yang, K. Novel Antibacterial Metals as Food Contact Materials: A Review. *Materials* **2023**, *16*, 3029, doi:10.3390/ma16083029.
22. de Larios, J.M.; Zhang, J.; Zhao, E.; Gockel, T.; Ravkin, M. Evaluating Chemical Mechanical Cleaning Technology for Post-CMP Applications. In Proceedings of the Micro; 1997; Vol. 15, p. 6.
23. Toure, Y.; Mabon, N.; Sindic, M. Soil Model Systems Used to Assess Fouling, Soil Adherence and Surface Cleanability in the Laboratory: A Review. *Biotechnologie, Agronomie, Société et Environnement* **2013**, *17*, 527–539.
24. Chen, Y.L.; Zhu, S.M.; Lee, S.J.; Wang, J.C. The Technology Combined Electrochemical Mechanical Polishing. *J. Mater. Process. Technol.* **2003**, *140*, 203–205, doi:10.1016/S0924-0136(03)00826-4.
25. Memisi, N.; Moracanin, S.V.; Milijasevic, M.; Babic, J.; Djukic, D. CIP Cleaning Processes in the Dairy Industry. *Procedia Food Science* **2015**, *5*, 184–186, doi:10.1016/j.profoo.2015.09.052.
26. Fryer, P.J.; Christian, G.K.; Liu, W. How Hygiene Happens: Physics and Chemistry of Cleaning. *International Journal of Dairy Technology* **2006**, *59*, 76–84, doi:10.1111/j.1471-0307.2006.00249.x.
27. Orihuel, E.; Bertó, R.; Lorenzo, F.; López, C. Mechanical Energy Balance in Surface Cleaning by Pressurised Water Spray : A Simplified Model. In *EHEDG Yearbook*; 2017; pp. 32–37.
28. Padmanabhan, N.T.; John, H. Titanium Dioxide Based Self-Cleaning Smart Surfaces: A Short Review. *J. Environ. Chem. Eng.* **2020**, *8*, 104211, doi:10.1016/j.jece.2020.104211.
29. Leclercq-Perlat, M.-N.; Lalande, M. Cleanability in Relation to Surface Chemical Composition and Surface Finishing of Some Materials Commonly Used in Food Industries. *Journal of Food Engineering* **1994**, *23*, 501–517, doi:10.1016/0260-8774(94)90108-2.
30. Köhler, H.; Stoye, H.; Mauermann, M.; Weyrauch, T.; Majschak, J.-P. How to Assess Cleaning? Evaluating the Cleaning Performance of Moving Impinging Jets. *Food and Bioproducts Processing* **2015**, *93*, 327–332, doi:10.1016/j.fbp.2014.09.010.
31. Lang, M.P.; Kocaoglu-Vurma, N.A.; Harper, W.J.; Rodriguez-Saona, L.E. Multicomponent Cleaning Verification of Stainless Steel Surfaces for the Removal of Dairy Residues Using Infrared Microspectroscopy. *J Food Sci* **2011**, *76*, C303-308, doi:10.1111/j.1750-3841.2010.02021.x.
32. Schöler, M.; Fuchs, T.; Helbig, M.; Augustin, W.; Scholl, S.; Majschak, J.-P. Monitoring of the Local Cleaning Efficiency of Pulsed Flow Cleaning Procedures.; 2009.
33. G. Detry, J.; Deroanne, C.; Sindic, M. Hydrodynamic Systems for Assessing Surface Fouling, Soil Adherence and Cleaning in Laboratory Installations. *Biotechnol. Agron. Soc. Environ.* **2009**, *13*, 427–439.
34. Davidson, C.A.; Griffith, C.J.; Peters, A.C.; Fielding, L.M. Evaluation of Two Methods for Monitoring Surface Cleanliness—ATP Bioluminescence and Traditional Hygiene Swabbing. *Luminescence* **1999**, *14*, 33–38, doi:10.1002/(SICI)1522-7243(199901/02)14:1<33::AID-BIO514>3.0.CO;2-I.
35. Rizzotto, F.; Khalife, M.; Hou, Y.; Chaix, C.; Lagarde, F.; Scaramozzino, N.; Vidic, J. Recent Advances in Electrochemical Biosensors for Food Control. *Micromachines* **2023**, *14*, 1412, doi:10.3390/mi14071412.
36. Yang, S.; Gao, S.; Zhuang, Y.; Hu, W.; Zhao, J.; Yi, Z. Non-Destructive Sensor for Glucose Solution Concentration Detection Using Electromagnetic Technology. *Micromachines* **2024**, *15*, 758, doi:10.3390/mi15060758.
37. Assaifan, A.K. Thiol-SAM Concentration Effect on the Performance of Interdigitated Electrode-Based Redox-Free Biosensors. *Micromachines* **2024**, *15*, 1254, doi:10.3390/mi15101254.

38. de Oliveira Krambeck Franco, M.; Suarez, W.T.; Santos, V.B. dos Digital Image Method Smartphone-Based for Furfural Determination in Sugarcane Spirits. *Food Anal. Methods* **2017**, *10*, 508–515, doi:10.1007/s12161-016-0605-4.
39. Agrisuelas, J.; García-Jareño, J.J.; Perianes, E.; Vicente, F. Use of RGB Digital Video Analysis to Study Electrochemical Processes Involving Color Changes. *Electrochem. Commun.* **2017**, *78*, 38–42, doi:10.1016/j.elecom.2017.04.001.
40. Minz, P.S.; Sawhney, I.K.; Saini, C.S. Algorithm for Processing High Definition Images for Food Colourimetry. *Measurement* **2020**, *158*, 107670, doi:10.1016/j.measurement.2020.107670.
41. Agrisuelas, J.; García-Jareño, J.J.; Vicente, F. Quantification of Electrochromic Kinetics by Analysis of RGB Digital Video Images. *Electrochem. Commun.* **2018**, *93*, 86–90, doi:10.1016/j.elecom.2018.06.011.
42. Kanchi, S.; Sabela, M.I.; Mdluli, P.S.; Inamuddin; Bisetty, K. Smartphone Based Bioanalytical and Diagnosis Applications: A Review. *Biosensors and Bioelectronics* **2018**, *102*, 136–149, doi:10.1016/j.bios.2017.11.021.
43. Agrisuelas, J.; García-Jareño, J.J.; Guillén, E.; Vicente, F. RGB Video Electrochemistry of Copper Electrodeposition/Electrodissolution in Acid Media on a Ternary Graphite:Copper:Polypropylene Composite Electrode. *Electrochim. Acta* **2019**, *305*, 72–80, doi:10.1016/j.electacta.2019.03.016.
44. Agrisuelas, J.; García-Jareño, J.J.; Guillén, E.; Vicente, F. Kinetics of Surface Chemical Reactions from a Digital Video. *J. Phys. Chem. C* **2020**, *124*, 2050–2059, doi:10.1021/acs.jpcc.9b10689.
45. Fan, Y.; Li, J.; Guo, Y.; Xie, L.; Zhang, G. Digital Image Colorimetry on Smartphone for Chemical Analysis: A Review. *Measurement* **2021**, *171*, 108829, doi:10.1016/j.measurement.2020.108829.
46. Agrisuelas, J.; García-Jareño, J.J.; Vicente, F. A Statistical Interpretation of the Voltammetry of Adsorbed Substances under the Perspective View of the Digital Video Electrochemistry. *Microchemical Journal* **2022**, *181*, 107844, doi:10.1016/j.microc.2022.107844.
47. Cánovas-Saura, A.; Serrano-Luján, L.; Beltrán, V.; Padilla, J. Neural Network-Based Digital Camera Spectrophotometer: Application to Chromogenic Technologies Characterization. *ACS Appl. Opt. Mater.* **2024**, *2*, 1403–1412, doi:10.1021/acsaom.4c00180.
48. García-Jareño, J.J.; Agrisuelas, J.; Vargas, Z.; Vicente, F. Electrogenation and Characterization of Poly(Methylene Blue) Thin Films on Stainless Steel 316 Electrodes—Effect of pH. *Molecules* **2024**, *29*, 3752, doi:10.3390/molecules29163752.
49. García-Jareño, J.J.; Agrisuelas, J.; Vicente, F. Overview and Recent Advances in Hyphenated Electrochemical Techniques for the Characterization of Electroactive Materials. *Materials* **2023**, *16*, 4226, doi:10.3390/ma16124226.
50. Agrisuelas, J.; García-Jareño, J.J.; Piedras, M.; Vicente, F. Quality and Efficiency Control of Electrodeposition and Electrodissolution of Ni on a Ternary Composite Electrode Followed by Digital Video Electrochemistry. *J. Electrochem. Soc.* **2023**, *170*, 072505, doi:10.1149/1945-7111/ace4f6.
51. Christeyns - Striving for a Cleaner Future Available online: <https://www.christeyns.com/> (accessed on 3 November 2023).

Disclaimer/Publisher's Note: The statements, opinions and data contained in all publications are solely those of the individual author(s) and contributor(s) and not of MDPI and/or the editor(s). MDPI and/or the editor(s) disclaim responsibility for any injury to people or property resulting from any ideas, methods, instructions or products referred to in the content.